

*Building structures are very often operated under the action of dynamic loads, both natural and man-made. The calculation of structures under the influence of static loads has been quite widely studied in detail. When structures are exposed to dynamic loads, additional tests are carried out, where measuring instruments are installed on the structures to register stresses and deformations that occur during dynamic influences. Elastic elements are the responsible functional unit of many measuring instruments. Therefore, the quality of elastic elements ensures the operational stability of the entire structure. This determines the increased attention that is paid to technology and construction to elastic elements. Previously, the work of elastic elements made of homogeneous mono materials with the same physical and geometric properties in all directions and over the entire surface of the element was studied.*

*The elastic element was considered as a shell of rotation with a complex shape of the meridian and various physical and mechanical properties at various points caused by uneven reinforcement. Two types of reinforcement were implied – radial and circular. Elastic shell elements (ESE) operate under conditions of dynamic loading. The equation was derived for determining the dynamic characteristics of inhomogeneous elastic elements. The dependences of the first three natural frequencies of oscillations on the thickness of the shell and the depth of the corrugation and the first two natural frequencies of oscillations on the thickness of the shell have been analyzed. The amplitude-frequency characteristics (AFC) and the phase-frequency characteristics (PFC) of the shell depending on the geometric parameters have been calculated. All these results could significantly improve the quality of the readings of the instruments, which depend on the sensitivity of the shell elastic elements. And it, in turn, depends on the geometric and physical properties of the shell elastic elements*

*Keywords: phase-frequency characteristics (PFC), amplitude-frequency characteristics (AFC), shell elastic elements (SEE), boundary conditions, geometric parameters*

# DETERMINING THE DYNAMIC CHARACTERISTICS OF ELASTIC SHELL STRUCTURES

**Irina Polyakova**

PhD\*

**Raikhan Imambayeva**

PhD\*

**Bakyt Aubakirova**

Corresponding author

PhD\*

E-mail: aubakirova.baxyt@mail.ru

\*Faculty of General Construction

Kazakh Leading Academy of Architecture and Civil Engineering

Ryskulbekova str., 28, Almaty, Republic of Kazakhstan, 050043

Received date 28.10.2021

Accepted date 08.12.2021

Published date 21.12.2021

**How to Cite:** Polyakova, I., Imambayeva, R., Aubakirova, B. (2021). Determining the dynamic characteristics of elastic shell structures. *Eastern-European Journal of Enterprise Technologies*, 6 (7 (114)), 43–51.

doi: <https://doi.org/10.15587/1729-4061.2021.245885>

## 1. Introduction

The operational reliability of structures in general and individual structural elements, in particular, is determined by the reliability of the elastic elements of various devices that make up the structural elements, and, consequently, the degree of accuracy of their work.

Environmental influences are often of a pronounced dynamic nature.

Therefore, due to the ever-increasing need for devices with elastic elements operating under various dynamic modes, it is a relevant task to study dynamic characteristics and calculate, based on them, the elastic shell elements [1, 2].

The relevance of our research is in the development of a methodology for determining the dynamic characteristics of ESE, the analysis of the impact of changes in the parameters of ESE geometry on their dynamic characteristics. All this could make it possible to construct elastic elements with more accurate results of work, as well as design them with the required characteristics.

## 2. Literature review and problem statement

A wide class of elastic elements (EE) consists of elastic elements such as thin-walled shells of rotation, in particular

corrugated, whose meridional cross-section is a wave-like curve. Such shells can be fabricated by applying concentric ring corrugations of arbitrary shape to any surface of rotation, termed the initial or main one. Paper [1] deals with the theory of calculating multilayer shells made of isotropic materials. The shells are considered smooth, and anisotropy is caused by a combination of different materials. However, shells with an arbitrary meridian shape are not considered. Work [2] examines elastic elements in the form of thin-walled shells of rotation with the shape of a meridian in the form of corrugations of various depths but consisting of mono materials. Such EEs have the same physical and mechanical properties in all directions. However, stresses in the EEs are determined only at static loads. Paper [3] determined elastic constants, taking into consideration the heterogeneity of the shells caused by uneven reinforcement. Refined values of such characteristics are used in research. Paper [4] sets out the provisions of finite-element methods for the calculation of a thin two-layer conical shell under the action of a uniformly distributed load using an axisymmetric finite element. The discrepancy between the results of the study of the proposed mathematical model and the available results of calculations using analytical formulas for thin two-layer conical shells does not exceed 9.3%. From a mathematical point of view, the finite-element method is widely implemented in the calculation of building structures. How-

ever, taking into consideration the uneven distribution of elastic characteristics in the calculation of heterogeneous corrugated shells could be very difficult to express when filling in the initial data, which makes this method difficult. Paper [5] addresses the issue of the calculation of multilayer structures by the type of layered plates and shells. The authors analyze the existing approaches in the field of calculation of layered plates and shells. It is established that the calculation of multilayer structures is considered using two main procedures: the theory of elasticity and the methods of mechanics of composite materials. The isotropic, anisotropic, and orthotropic structures of the plates and shells, which obey Hooke's law, were considered. The choice of calculation methodology depends on the composition of the multilayer structure, the rigidity of the middle layer, and the diverse orientation of all layers. Studies of the stressed-strained state and the distribution of forces between the components of multilayer structures in the above calculations show that the deformation state is mainly described by Hooke's generalized law. An important factor is to take into consideration the general anisotropy of the structure and the work of the middle layer in the layered structure. However, shells with a complex shape of the meridian and shells with anisotropy caused by uneven reinforcement were not considered. In [6], the same structures are considered but the SCAD program (RF) is used. A comparison of theoretical and computer calculations is given. For the same reasons that were specified regarding the finite-element method (FEM), this method is not desirable in the calculation of SEE.

Paper [7] reports determining the natural oscillations of cylindrical shells made of composites. However, composites are assumed to be various combinations of plastic materials, rather than matrix-reinforcing fiber combinations. Study [8] considers various types of composites for use in building structures, but without the calculation of specific structural elements for dynamic effects. Work [9] considers the oscillations of the shell. Based on the variational Lagrange equation, certain tests of a viscoelastic ribbed truncated conical shell are obtained. Based on the finite element method, methods of solving and equations of proper oscillations of a viscoelastic ribbed truncated conical shell with articulated and freely operated edges are used. The problem is reduced to solving homogeneous algebraic equations with complex coefficients of a large order. However, that shell is homogeneous, with a simple meridian shape. In [10], the author describes the conditions of generalized orthogonality of the oscillation shapes of an elastic dissipative system, for which the traditional classical orthogonality conditions are a special case. Within the framework of the theory of temporal analysis, the shapes of free oscillations of an elastic-plastic system are built on the basis of the use of a schematic diagram of deformation with strengthening. However, the cited paper does not consider the dynamic characteristics that depend on the geometry of the structure. Paper [11] states the initial boundary problem of viscoelastic bending of cylindrical round shells transversely reinforced on equidistant surfaces. Instantaneous elastic-plastic deformation of the components of the shell is described by the basic equations from the theory of plastic flow with isotropic hardening. However, the dynamics of rotation shells made of composite materials are not considered. Study [12] discusses the multilayer shell and identifies stresses and deformations. However, the anisotropy of such shells is caused by different materials of the layers, and not by reinforcing fibers. Work [13] considers the tensile

forces of the toroidal shell caused by pressure and rotation, as well as their effect on their natural oscillations. However, dynamic forces are not taken into consideration and heterogeneous shells are ignored. Paper [14] covers the stability of parametric oscillations in the shape of a hyperbolic paraboloid but does not consider the shells of rotation and determining the dynamic characteristics. In [15], a numerical analysis of nonlinear forced oscillations of a cylindrical shell with a combinational internal resonance in a fractional viscoelastic medium was performed. However, the dynamics of rotation shells made of composite materials are not touched upon. Study [16] considers nonlinear oscillations of a cylindrical shell of a layered polymer reinforced with carbon fiber. However, other combinations of composite materials were not analyzed, for example, a metal matrix and a stiffer metal fiber. The shell was considered as simple cylindrical rather than a rotational shell. Paper [17] determines the influence of the parameters of the non-constant load on the transient process of oscillations of the ribbed cylindrical shell. However, the operation of rotation shells under the action of a dynamic load was not taken into consideration. In [18], a new shell element with double curvature for free oscillations of layered structures of arbitrary shape was calculated on the basis of isogeometric analysis. However, the issues of oscillations of heterogeneous shells unevenly reinforced with metal fibers were not considered. The review of literary sources allows us to assert that it is advisable to conduct a study aimed at determining the dynamic characteristics of the structures of heterogeneous shells of rotation under various influences.

---

### 3. The aim and objectives of the study

---

The purpose of this study is to analyze the effect of changes in the geometric parameters of ESE on the main dynamic characteristics. Our theoretical studies could make it possible to design elastic shell elements with the predefined dynamic characteristics, as well as to improve the accuracy of the measured values.

To accomplish the aim, the following tasks have been set:

- to draw up a design scheme of the elastic element as a shell of rotation under deformation and build an equilibrium equation;
- to derive equations for determining the frequencies and shapes of the free oscillations of corrugated shell EEs;
- to bring the system of equations to a dimensionless form and to define boundary conditions;
- to determine the displacements and stresses during the forced oscillations of corrugated EEs under the influence of arbitrary external loads.

---

### 4. The study materials and methods

---

Addressing the first three tasks makes it possible to establish the dependences of the natural frequencies and shapes of an elastic element on the main design parameters, and, consequently, enables the design of elements with the predefined natural frequencies.

When tackling the fourth task, forced fluctuations of EE are considered under harmonic, unit pulse, unit step, and other external influences, which makes it possible to determine the AFC, PFC, pulse, and transition characteristics of the element and establish their dependence on the main design parameters.

To perform the study, a dynamic model was adopted, which makes it possible to calculate the dynamic characteristics of SEE with an arbitrary shape of the meridian. In deriving the system of equations, the validity of the Kirchhoff-Love hypotheses was allowed. The oscillations were considered small, the EE was considered a rotation shell with a rigid center, and all accepted assumptions correspond to the actual operating conditions of SEE. The external static load is replaced by the sum of the intensities of the inertial forces and the viscous friction forces. A system of partial differential equations describing the forced oscillations of the shell under the action of a harmonic load is built. The solution to the system of equations was expanded into a Fourier series for time and angle in the circumferential direction. A transition to the original system of ordinary linear differential equations with variable coefficients is carried out. When considering free oscillations, the original system was brought to a homogeneous form. The derivation of boundary conditions is given.

Since the resulting system of differential equations does not have a common solution, the integration was carried out by the numerical method according to a specially developed software, based on the specificity of the process under consideration. To integrate the original system of differential equations, the classical predictor-corrector Hamming method with automatic selection of the integration step was chosen. In order to avoid "flattening" the vectors of solutions, the method of orthogonalization of solutions at intermediate points of integration, proposed by S. K. Godunov, was applied.

To implement the algorithm for the numerical calculation of the dynamic characteristics of EE, the frequency of natural and forced oscillations, a calculation subprogram was compiled.

## 5. Results of the development of a methodology for determining the dynamic characteristics of elastic shells

### 5.1. Justification of the estimation scheme

The estimation scheme of the median surface of an elastic element is considered as a thin-walled shell of rotation with an arbitrary meridian (Fig. 1).

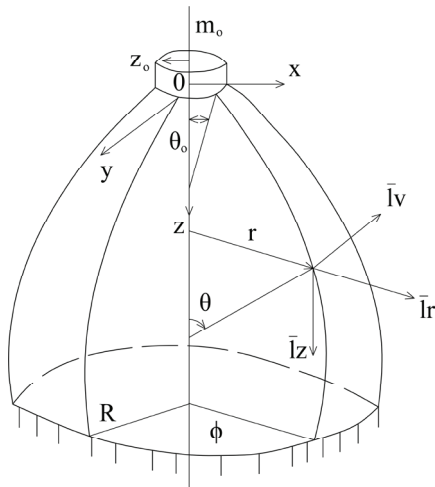


Fig. 1. The estimation scheme of an element

The law of changing the thickness of the shell along the meridian is arbitrary. We believe that the material of the

shell obeys the generalized Hooke's law. The median surface of the shell is assigned to the Gaussian coordinates \$s\$ and \$\phi\$. One edge of the shell (\$s=0, \theta=\theta\_0\$) is connected to an absolutely rigid flange of radius \$r\_0\$ and mass \$m\_0\$, the other edge (\$s=s\_k, \theta=\theta\_k\$) is rigidly sealed. For the main unknowns, let us take the components of the vector of displacements: \$u\_r, u\_z, v, \vartheta\$ and the vectors of internal forces: \$Q\_r, Q\_z, S^\*, M\_1\$, related to the coordinate system \$(r, z, v)\$, which are functions of the variables \$s, \phi, t\$.

The following notations are introduced here:

- \$u\_r\$ is the radial displacement;
- \$u\_z\$ is the axial displacement;
- \$v\$ is the circumferential displacement of an arbitrary point at the surface of the tin;
- \$\vartheta\$ is the angle of rotation of the normal to the median surface in the meridional plane;
- \$Q\_r\$ is the radial force;
- \$Q\_z\$ is the axial force;
- \$S^\*\$ is the reduced shear force at an arbitrary point of the shell, related to the unit length of the parallel;
- \$M\_1\$ is the meridional bending momentum at an arbitrary point of the shell, related to the unit length of the parallel;
- \$s\$ is the arc length of the shell meridian, counted from the outer contour of the rigid center;
- \$\phi\$ is the angle between the initial meridian and the meridian passing through an arbitrary point of the median surface (Fig. 4);
- \$\theta\$ is the angle of inclination of the normal of the undeformed median surface to the axis of the shell;
- \$R\$ is the overall radius of the shell;
- \$m\_0\$ is the mass of the rigid center;
- \$r\_0\$ is the radius of the rigid center;
- \$r\$ is the radius of the parallel circle;
- \$h\$ is the thickness of the shell.

### 5.2. Derivation of equations for determining the frequencies and shapes of free oscillations of corrugated shell elastic elements

After drawing up the equations of equilibrium and mathematical transformations, the following system of equations is built:

$$\begin{aligned} \frac{du_r}{ds} &= -v_1 E_1 \frac{\cos \theta}{r} u_r - v_1 \frac{E_2 \cos \theta}{E_1 r} \frac{\partial v}{\partial \phi} - \sin \theta \vartheta + \\ &+ \frac{1-v_1 v_2 \cos^2 \theta}{E_1 h} Q_r + \frac{1-v_1 v_2 \sin \theta \cos \theta}{E_1 h} Q_z, \\ \frac{du_z}{ds} &= -v_1 \frac{E_2 \sin \theta}{E_1 r} u_r - v_1 \frac{E_2 \sin \theta}{E_1 r} \frac{dv}{d\phi} - \cos \theta \vartheta + \\ &+ \frac{1-v_1 v_2 \sin \theta \cos \theta}{E_1 h} Q_r + \frac{1-v_1 v_2 \sin^2 \theta}{E_1 h} Q_z, \\ \frac{dv}{ds} &= -\frac{\cos \theta}{r} \frac{\partial u_r}{\partial \phi} - \frac{\sin \theta}{r} \frac{\partial u_z}{\partial \phi} + \\ &+ \frac{\cos \theta}{r} v - \frac{h^2}{3r^2} \sin \theta \frac{\partial \vartheta}{\partial \phi} + \frac{2(1+v_1)}{E_1 h} S^*, \\ \frac{d\vartheta}{ds} &= -v_1 \frac{E_2 \cos \theta}{E_1 r} \vartheta + \frac{12(1-v_1 v_2)}{E_1 h^3} M_1 - \\ &- v_1 \frac{E_2 \sin \theta}{E_1 r^2} \frac{\partial^2 u_r}{\partial \phi^2} + v_1 \frac{E_2 \cos \theta}{E_1 r^2} \frac{\partial^2 u_z}{\partial \phi^2} + v_1 \frac{E_2 \sin \theta}{E_1 r^2} \frac{\partial v}{\partial \phi}, \end{aligned} \tag{1}$$

$$\begin{aligned} \frac{dQ_r}{ds} &= \frac{E_2 h}{r^2} u_r - \frac{E_2 h}{r^2} \frac{\partial v}{\partial \varphi} - \frac{E_2 h^3}{12 r^3} \sin \theta \cos \theta \frac{\partial^2 \vartheta}{\partial \varphi^2} - \\ &- (1 - \nu_2) \frac{\cos \theta}{r} Q_r + \nu_2 \frac{\sin \theta}{r} Q_z - \\ &- \frac{\cos \theta}{r} \frac{\partial S^*}{\partial \varphi} + \nu_2 \frac{\sin \theta}{r} \frac{\partial^2 M_1}{\partial \varphi^2} - q_r, \\ \frac{dQ_z}{ds} &= - \frac{E_2 h^3}{6(1 + \nu_2) r^4} \frac{\partial^2 u_z}{\partial \varphi^2} + \frac{E_2 h^3}{6(1 + \nu_2) r^3} \frac{\partial^2 \vartheta}{\partial \varphi^2} + \\ &+ \frac{E_2 h^3 \cos^3 \theta}{12 r^3} \frac{\partial^2 \vartheta}{\partial \varphi^2} - \frac{\cos \theta}{r} Q_z - \\ &- \frac{\sin \theta}{r} \frac{\partial S^*}{\partial \varphi} + \nu_2 \frac{\cos \theta}{r^2} \frac{\partial^2 M_1}{\partial \varphi^2} - q_z, \\ \frac{dS^*}{ds} &= - \frac{E_2 h}{r^2} \frac{\partial u_r}{\partial \varphi} - \frac{E_2 h}{r^2} \frac{\partial^2 v}{\partial \varphi^2} - \\ &- \frac{E_2 h^3 \sin \theta \cos \theta}{12 r^3} \frac{\partial \vartheta}{\partial \varphi} + \nu_2 \frac{\cos \theta}{r} \frac{\partial Q_r}{\partial \varphi} + \\ &+ \nu_2 \frac{\sin \theta}{r} \frac{\partial Q_z}{\partial \varphi} - 2 \frac{\cos \theta}{r} S^* + \nu_2 \frac{\sin \theta}{r} \frac{\partial M_1}{\partial \varphi} - q_v, \\ \frac{dM_1}{ds} &= - \frac{E_2 h^3 \sin \theta \cos \theta}{12 r^3} \frac{\partial^2 u_r}{\partial \varphi^2} + \frac{E_2 h^3 \cos \theta}{12 r^3} \frac{\partial^2 u_z}{\partial \varphi^2} + \\ &+ \frac{E_2 h^3}{6(1 + \nu_2) r^3} \frac{\partial^2 u_z}{\partial \varphi^2} + \frac{E_2 h^3 \sin \theta \cos \theta}{12 r^3} \frac{dv}{d\varphi} + \\ &+ \frac{E_2 h^3}{12} \cos \theta^* \vartheta - \frac{E_2 h^3}{6(1 + \nu_2) r^2} \frac{\partial^2 \vartheta}{\partial \varphi^2} + \sin \theta^* Q_r - \\ &- \cos \theta^* Q_z - \frac{h^2 \sin \theta}{3 r^2} \frac{dS^*}{d\varphi} - (1 - \nu_2) \frac{\cos \theta}{r} M_1, \end{aligned}$$

where:

- $u_r = u_r(\varphi, s, t)$ ,  $u_z = u_z(\varphi, s, t)$ ,  $v = v(\varphi, s, t)$ ,  $\vartheta = \vartheta(\varphi, s, t)$  – displacements;
- $Q_r = Q_r(\varphi, s, t)$ ,  $Q_z = Q_z(\varphi, s, t)$ ,  $S^* = S^*(\varphi, s, t)$ ,  $M_1 = M_1(\varphi, s, t)$  – forces;
- $h$  is the shell thickness;
- $q_r = q_r(\varphi, s, t)$ ,  $q_z = q_z(\varphi, s, t)$ ,  $q_v = q_v(\varphi, s, t)$  is the intensity of inertial and pressure forces in the radial, axial, and circumferential directions.

The mechanical characteristics in the direction of axes 1 (along the radius) and 2 (perpendicular to the radius) depend on the location of the reinforcing fibers and are equal to:

$$\begin{aligned} E_1 &= E_B \Psi_B(r_0) \frac{r_0}{r} + E_M \left[ 1 - \Psi_B(r_0) \frac{r_0}{r} \right], \\ E_2 &= \frac{E_m}{\Psi_B(r_0) \frac{r_0}{r} \frac{E_M}{E_B} + \left[ 1 - \Psi_B(r_0) \frac{r_0}{r} \right]}, \\ \nu_1 &= \Psi_B(r_0) \frac{r_0}{r} \nu_B + \left[ 1 - \Psi_B(r_0) \frac{r_0}{r} \right] \nu_M, \\ \nu_2 &= \frac{\nu_1 E_2}{E_1}. \end{aligned}$$

If we take into consideration the refined value of the modulus of elasticity [3], then the parameter  $E_2$  is calculated:

$$\begin{aligned} E_2 &= \frac{E_m}{1 - e} \left[ \frac{\frac{\pi}{2} + \arcsin \left[ 2\sqrt{\Psi(1 - e)} \right]}{\sqrt{1 - \frac{4\Psi(1 - e^2)}{\pi}}} - \frac{\pi}{2} \right] + \\ &+ E_M \left( 1 - 2\sqrt{\frac{\Psi}{\pi}} \right). \end{aligned}$$

The refined values of modulus of elasticity and Poisson coefficients were obtained for shells reinforced along the radius and along the ring.

### 5.3. Bringing the system of equations to dimensionless form and determining boundary conditions

To calculate the free and forced oscillations of the shell elastic elements, it is advisable to represent equations (1) in a dimensionless form. To this end, the following dimensionless parameters are introduced:

$$\begin{aligned} x &= \frac{s_1 - s}{R}; \quad y_1 = \frac{u_{rks}^{(k)}}{R}; \quad y_2 = \frac{u_{rkc}^{(k)}}{R}; \quad y_3 = \frac{u_{zks}^{(k)}}{R}; \\ y_4 &= \frac{u_{zkc}^{(k)}}{R}; \quad y_5 = \frac{v_{ks}^{(k)}}{R}; \quad y_6 = \frac{v_{kc}^{(k)}}{R}; \quad y_7 = \frac{v_{ks}^{(k)}}{2\pi}; \\ y_8 &= \frac{v_{kc}^{(k)}}{2\pi}; \quad y_9 = \frac{Q_{rks}^{(k)}}{Eh_0}; \quad y_{10} = \frac{Q_{rkc}^{(k)}}{Eh_0}; \quad y_{11} = \frac{Q_{zks}^{(k)}}{Eh_0}; \\ y_{12} &= \frac{Q_{zkc}^{(k)}}{Eh_0}; \quad y_{13} = \frac{S_{ks}^{*(k)}}{Eh_0}; \quad y_{14} = \frac{S_{kc}^{*(k)}}{Eh_0}; \quad y_{15} = \frac{M_{1ks}^{(k)}}{Eh_0^2}; \\ y_{16} &= \frac{M_{1kc}^{(k)}}{Eh_0^2}; \quad \lambda = \frac{p}{p_0}; \quad l = \frac{r}{R}, \end{aligned} \tag{2}$$

where  $p_0$ ,  $h_0$  are the normalizing multipliers of the frequency of oscillations and the thickness of the shell, the choice of the value for which is dictated by the specific conditions of the problem being solved. By introducing notation (2), the system of ordinary differential equations with respect to the amplitudes of the components of displacements and forces can be written in the following vector form:

$$\frac{d}{dx} \bar{y} = A \bar{y} + \bar{q}, \tag{3}$$

where  $\bar{y}$  is the state vector with components  $y_1, y_2, \dots, y_{16}$ ;

$A$  is the square matrix of variable coefficients;

$\bar{q}$  is the load vector.

Numerical methods are used to solve the system (1) since an analytical solution is almost impossible. Solutions to equations (1) in harmonic perturbation can be represented as:

$$\begin{aligned} u_r(\varphi, s, t) &= \left( u_{rks}^{(k)} \sin pt + u_{rkc}^{(k)} \cos pt \right) \cos k\varphi; \\ u_z(\varphi, s, t) &= \left( u_{zks}^{(k)} \sin pt + u_{zkc}^{(k)} \cos pt \right) \cos k\varphi; \\ v(\varphi, s, t) &= \left( v_{ks}^{(k)} \sin pt + v_{kc}^{(k)} \cos pt \right) \cos k\varphi; \\ \nu(\varphi, s, t) &= \left( \nu_{ks}^{(k)} \sin pt + \nu_{kc}^{(k)} \cos pt \right) \cos k\varphi; \\ Q_r(\varphi, s, t) &= \left( Q_{rks}^{(k)} \sin pt + Q_{rkc}^{(k)} \cos pt \right) \cos k\varphi; \end{aligned} \tag{4}$$

$$Q_z(\phi, s, t) = (Q_{zks}^{(k)} \sin pt + Q_{zkc}^{(k)} \cos pt) \cos k\phi;$$

$$S^*(\phi, s, t) = (S_{ks}^{*(k)} \sin pt + S_{kc}^{*(k)} \cos pt) \cos k\phi;$$

$$M_1(\phi, s, t) = (M_{1ks}^{(k)} \sin pt + M_{1kc}^{(k)} \cos pt) \cos k\phi;$$

where  $k=0,1,2,3,\dots$

In (4), the lower and upper indices, at the constituent displacements and forces, are used to denote the values that are, respectively, symmetrical and obliquely symmetric relative to the initial meridian.

Similarly, the load acting on the shell can be represented:

$$q_r(\phi, s, t) = (q_{rks}^{(k)} \sin pt + q_{rkc}^{(k)} \cos pt) \sin k\phi;$$

$$q_z(\phi, s, t) = (q_{zks}^{(k)} \sin pt + q_{zkc}^{(k)} \cos pt) \sin k\phi; \quad (5)$$

$$q_v(\phi, s, t) = (q_{vks}^{(k)} \sin pt + q_{vkc}^{(k)} \cos pt) \sin k\phi.$$

The solution and load components on the right side of expressions (4) and (5) are  $s$  functions.

In these expressions:

–  $p$  is the frequency of change in the harmonic perturbation;

–  $k$  is half the value of the number of nodal meridians (the number of waves in the circumferential direction).

The derivation of boundary conditions was carried out as follows.

Solutions to the system of equations (1) must be subject to boundary conditions in two circumferential cross-sections bounding the shell (in general, eight conditions at each edge). Boundary conditions are imposed directly on the main unknown movements or their corresponding efforts [1].

For the calculation scheme under consideration (Fig. 1), at any values of  $k$ , it is obvious that at  $s=s_k$  ( $s_k$  is the final length of the arc of the meridian) all components of the displacements are zero:

$$\begin{aligned} u_{rks}^{(k)} = 0; \quad u_{rkc}^{(k)} = 0; \quad u_{zks}^{(k)} = 0; \quad u_{zkc}^{(k)} = 0; \\ v_{rks}^{(k)} = 0; \quad v_{rkc}^{(k)} = 0; \quad v_{zks}^{(k)} = 0; \quad v_{zkc}^{(k)} = 0; \\ (k = 0, 1, 2, \dots). \end{aligned} \quad (6)$$

Boundary conditions can now be formulated to satisfy the solutions to the system of equations (1) at  $s=0$ . To this end, the dynamic equilibrium of the rigid center (flange) is considered [2]. Let the center  $O$  of the flange move in the directions  $x, y, z$  at  $\Delta_x, \Delta_y, \Delta_z$ , respectively. Also, let the flange rotate relative to the axes at angles  $\psi_x, \psi_y, \psi_z$ . The vector of movement of an arbitrary point of the flange contour, under the condition of the smallness of movements and rotation angles, can be written as:

$$\bar{\xi} = \bar{\Delta} + \bar{\psi} \times \bar{r}. \quad (7)$$

Here

$$\bar{\Delta} = \Delta_x \bar{i} + \Delta_y \bar{j} + \Delta_z \bar{k};$$

$$\bar{\psi} = \psi_x \bar{i} + \psi_y \bar{j} + \psi_z \bar{k};$$

$$\bar{r} = r_0 \sin \phi \bar{i} + r_0 \cos \phi \bar{j},$$

where  $i, j, k$  are the orts of the  $x, y, z$  axes;  $r_0$  is the radius of the rigid center.

Writing (7) in the movements on the stationary axes  $x, y, z$ , we obtain:

$$\xi_x = \Delta_x - \psi_z r_0 \cos \phi;$$

$$\xi_y = \Delta_y - \psi_z r_0 \sin \phi; \quad (8)$$

$$\xi_z = \Delta_z + \psi_x r_0 \cos \phi - \psi_y r_0 \sin \phi.$$

Mapping the vector of movement of an arbitrary point of the end ( $s=0$ ) of the shell onto the  $x, y, z$  axes, we obtain:

$$\xi_x = u_r \sin \phi + v \cos \phi;$$

$$\xi_y = u_r \cos \phi - v \sin \phi; \quad (9)$$

$$\xi_z = u_z.$$

Expressing the unit vectors  $\bar{i}$  and  $\bar{j}$  through the unit vectors  $\bar{e}_r$  and  $\bar{e}_v$  on the contour of the flange, we obtain:

$$\bar{i} = \bar{e}_r \sin \phi + \bar{e}_v \cos \phi;$$

$$\bar{j} = \bar{e}_r \cos \phi - \bar{e}_v \sin \phi.$$

Thus, all equations are brought to a dimensionless form for the convenience of solving and compiling a calculation program.

#### 5. 4. Determining the displacements and stresses under the forced oscillations of corrugated elastic elements

Stresses:

$$\sigma_1 = \frac{T_1}{h} \pm \frac{6M_1}{h^2},$$

$$\sigma_2 = \frac{T_2}{h} \pm \frac{6M_2}{h^2}, \quad (10)$$

where  $\sigma_1, T_1, M_1$  are, respectively, the stress, force, and bending momentum in a cross-section perpendicular to the median surface;

$\sigma_2, T_2, M_2$  are, respectively, the magnitudes in the cross-section parallel to the meridional plane.

In (10), the plus sign is used for stresses on the compressed surface. The stress in the cross-section parallel to the median surface is neglected according to the accepted Kirchhoff-Love hypothesis. The force factors included in equations (10) are determined through the components of the state vector:

$$T_1 = Q_{or} \cos \theta + Q_{oz} \sin \theta;$$

$$M_1 = M_{01};$$

$$T_2 = Q_{or} \mu \cos \theta + Q_{oz} \mu \sin \theta + u_{or} \frac{Eh}{r}; \quad (11)$$

$$M_2 = \mu M_1 + v_{01} \frac{Eh^3}{12r} \cos \theta;$$

where

$$\begin{aligned}
 Q_{or} &= \sqrt{Q_{Ors}^2 + Q_{Orc}^2}; \\
 M_{o1} &= \sqrt{M_{10s}^2 + M_{10c}^2}; \\
 u_{or} &= \sqrt{u_{Ors}^2 + u_{Orc}^2}; \\
 v_{o1} &= \sqrt{v_{10s}^2 + v_{10c}^2}.
 \end{aligned}
 \tag{12}$$

The equivalent stress is determined from energy theory:

$$\sigma_{eqv} = \sqrt{\sigma_1^2 + \sigma_2^2 - \sigma_1 \sigma_2}.
 \tag{13}$$

Strength testing is carried out according to the following condition:

$$\sigma_{eqv} \leq [\sigma] = \frac{\sigma_T}{n_T},
 \tag{14}$$

where  $[\sigma]$  is the allowable stress;  $\sigma_T$  is the yield strength at stretching or compression;  $n_T$  is the yield factor.

Based on the calculation results, we constructed the plots showing the dependence of the first three frequencies of natural oscillations on the thickness of the shell (Fig. 2).

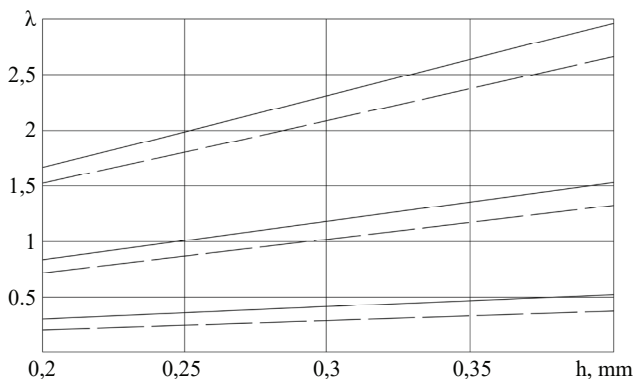


Fig. 2. Dependence of the first three natural frequencies of elastic elements on thickness:  $k=0$  – solid lines;  $k=1$  – dashed lines

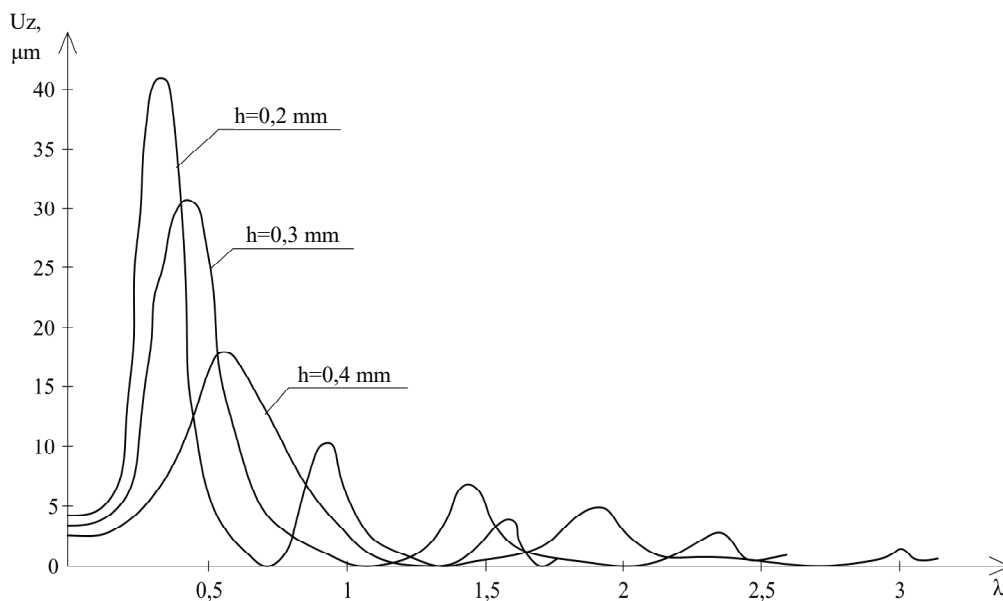


Fig. 5. Amplitude-frequency characteristics of the elastic element depending on the thickness of the shell

A plot of the dependence of the first three frequencies of natural oscillations on the depth of the corrugation is shown in Fig. 3.

Fig. 4 shows the dependence of the first two frequencies of elastic elements on the element thickness.

The amplitude-frequency characteristics of the elastic element depending on the thickness of the shell were derived (Fig. 5).

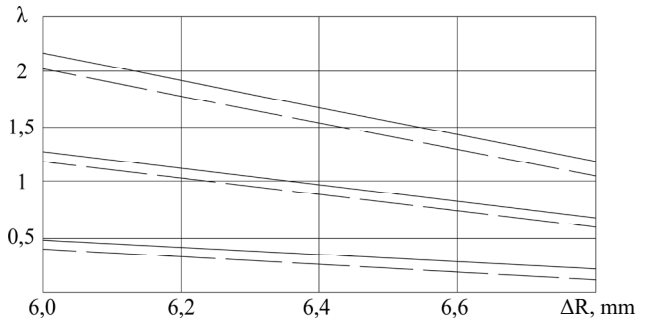


Fig. 3. The dependence of the first three natural frequencies of elastic elements on corrugation depth. For  $k=0$  – solid lines, for  $k=1$  – dashed lines

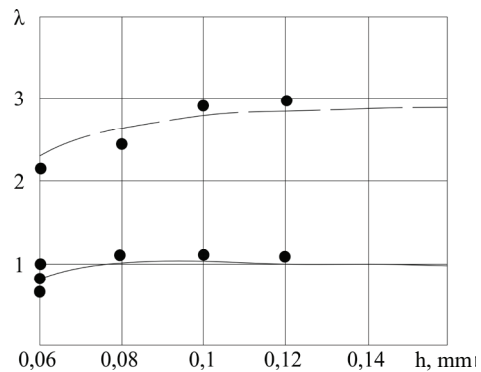


Fig. 4. The dependence of the first two frequencies of elastic elements on thickness: solid line – the first frequency, bar line – the second; points – frequencies determined experimentally

The phase-frequency characteristics of the elastic element, depending on its thickness, are shown in Fig. 6.

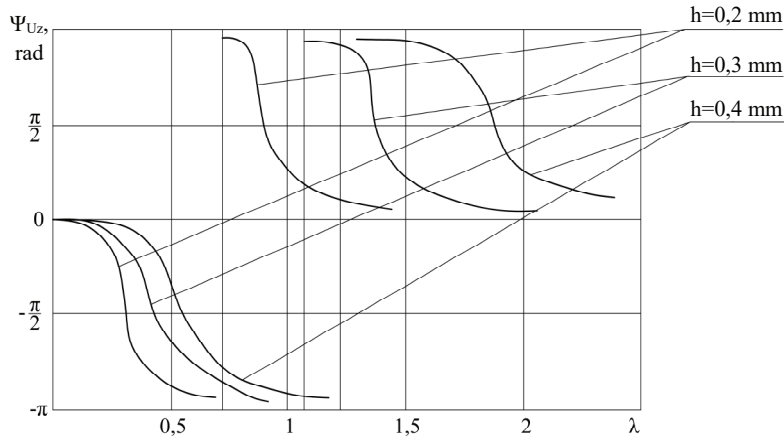


Fig. 6. Phase-frequency characteristics of the elastic element depending on its thickness

Fig. 7 shows the diagrams of equivalent stresses of an elastic element.

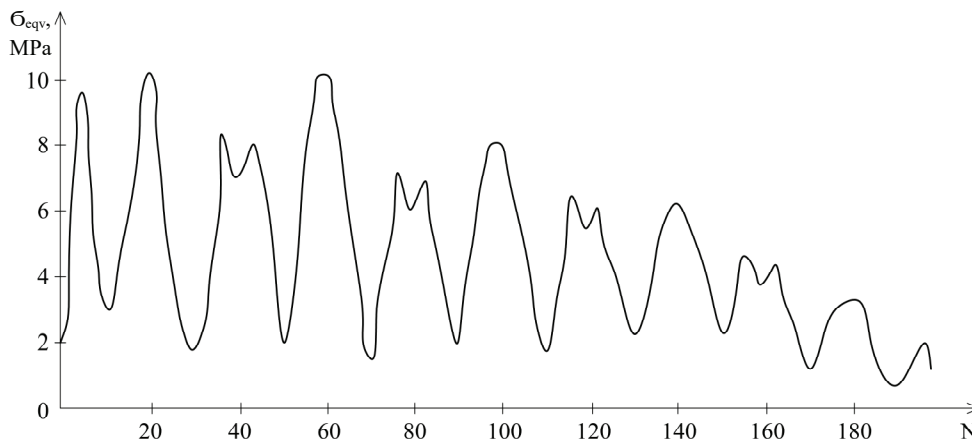


Fig. 7. Diagrams of equivalent stresses of the elastic element

The amplitude-frequency characteristics of the equivalent stress of the elastic element are shown in Fig. 8.

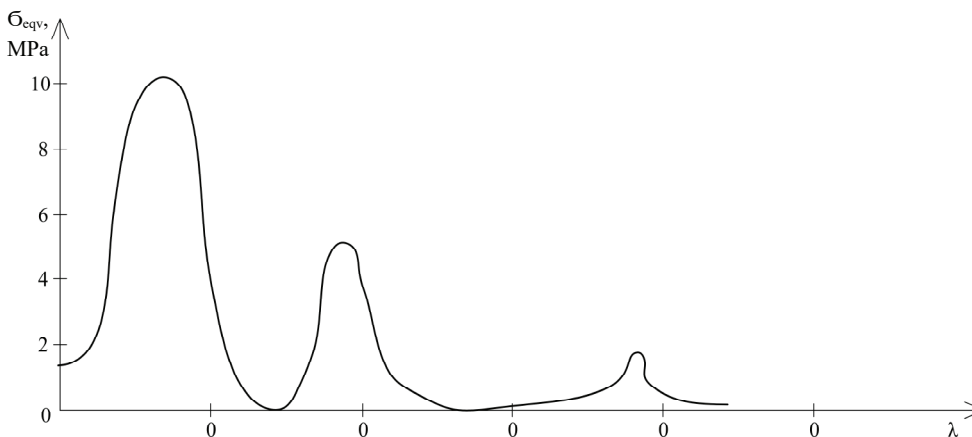


Fig. 8. Amplitude-frequency characteristics of the equivalent stress of the elastic element

Fig. 2–8 show plots of the dependences of oscillation frequencies, AFC, and PFC on geometric parameters, constructed as a result of our calculations.

### 6. Discussion of results of applying the methodology for determining the dynamic characteristics of elastic shells

The dependence of AFC, PFC, and stresses on the values of  $P_z$ ,  $R$ ,  $h$ ,  $\Delta R$  can be established by successively varying their values within the predefined limits.

Fig. 2–4 show the dependence of the first two natural frequencies of EE on the shell thickness  $h$ , with axisymmetric oscillations ( $k=0$ ), where  $0.06 \leq h \leq 0.16$  mm, the solid line – the first frequency, dash – the second, the points are the natural frequency determined experimentally.

Fig. 2, 3 demonstrate that all three considered first frequencies have the same pattern of change both depending on the thickness and depending on the depth of the corrugation. Namely, with increasing thickness, their values increase, and linearly, which is explained by an increase in the stiffness of ESE. With an increase in the depth of the corrugation, that is, with an increase in the outer radius, their values decrease, which is explained by a decrease in stiffness and an increase in mass.

Fig. 5 shows the EE PFC depending on its shell thickness. Analysis of the figure reveals that phase errors in the operating frequency range decrease with the increasing thickness of the EE.

Along with the metrological parameters discussed above, the characteristics that determine the strength and reliability of EE are of great importance. The most important of them is the magnitude of stresses in the considered EE.

Stresses in the EE have been determined. As an object of our study, the EE is taken whose geometric and mechanical characteristics are given in [8], under the action of an external acceleration field with an intensity of 1 g.

Fig. 7 shows the diagram of equivalent stresses in EE at the frequency of the external field of accelerations coinciding with the first natural frequency since the greatest stresses occur at resonance frequencies. Fig. 7 demonstrates that the tops and troughs of the SE corrugations are the most loaded. At the first natural frequency, the internal bends are loaded

weaker than the outer ones. Moreover, the nature of the distribution of equivalent stresses along the EE meridian is qualitatively the same as with static loading.

Fig. 8 shows the AFC of the maximum equivalent stress that occurs at the 20th point of orthogonalization, that is, at the apex of the first external bend. The maximum equivalent stress reaches the highest values at resonance frequencies.

The undoubted advantage of our proposed calculation method is the possibility to design SEE with the predefined characteristics, using various combinations of reinforcement and types of corrugation.

For the specific use of our study results aimed at obtaining a rational design solution for SEE, the following main stages must be performed:

- numerical calculation in order to obtain the dependences of the dynamic characteristics (performance indicators) of SEE on its design parameters;
- analysis of the obtained dependences, determining the degree of influence exerted on the dynamic characteristics by various design parameters of SEE, defining the necessary set of design parameters;
- analysis of the dependences of the dynamic characteristics of the SEE on its design parameters, taking into consideration the restrictions imposed on these characteristics, the construction of cross-sections of the corresponding areas of operability.

Further work on the implementation of our study results would make it possible to design SEE with the predefined geometric and physical characteristics, as well as improve the accuracy of the measured results.

---

## 7. Conclusions

---

1. We have built an estimation scheme of an elastic element as a shell of rotation under deformation and constructed a system of differential equations of shell equilibrium under dynamic action. A special feature of the proposed scheme

is that the shell is unevenly reinforced with metal fiber and has a complex shape of the meridian (corrugated).

2. Equilibrium equations have been compiled and a system of equations has been derived for determining the basic operating characteristics of ESE (natural frequencies, state vectors, AFC, PFC, and stresses), which make it possible to theoretically investigate the influence of the parameters of ESE geometry on these characteristics. A special feature of these equations is that they are built for heterogeneous shell elements. This heterogeneity is caused by the shape of the shell meridian (corrugated surface), as well as uneven reinforcement of the shell, which makes the values of the Poisson coefficients and modulus of elasticity different at each point of the shell.

3. The system of equations for calculating the free and forced oscillations of the shell elastic elements is reduced to a dimensionless form with the boundary conditions determined. A feature of the proposed solution to this system of equations, as a solution to the problem of dynamics of inhomogeneous shells of rotations with a complex meridian shape, is the application of the orthogonalization method. The main performance characteristics (AFC, PFC) have been determined, which makes it possible to theoretically investigate the influence of the parameters of SEE geometry on these characteristics.

4. We have determined the displacements, stresses of EE under dynamic loads. The dependences of the first three natural frequencies of the SEE on its thickness and the depth of the corrugation and the first two natural frequencies on its thickness have been established and analyzed. This analysis makes it possible to design SEE with predefined characteristics. The implementation of our study results could allow for the following:

- a decrease in the volume of selective assembly of units, by (15÷20) %;
  - a decrease in the node-related defects by (10÷15) %;
  - an improvement in the accuracy of units' operation by (20÷25) %.
- 

## References

1. Alfutov, N. A., Zinov'ev, P. A., Popov, B. (2009). Raschet mnogoslonykh plastin i obolochek iz kompozitsionnykh materialov. Moscow: Mashinostroenie, 263. Available at: [https://www.studmed.ru/alfutov-na-zinovev-pa-popov-bg-raschet-mnogoslonykh-plastin-i-obolochek-iz-kompozitsionnykh-materialov\\_a4d2eb5991d.html](https://www.studmed.ru/alfutov-na-zinovev-pa-popov-bg-raschet-mnogoslonykh-plastin-i-obolochek-iz-kompozitsionnykh-materialov_a4d2eb5991d.html)
2. Andreeva, L. E. (1962). Uprugie elementy priborov. Moscow: Mir knig, 462. Available at: <https://xn--c1ajahiit.ws/knigi/nehudozhestvennye/nauka-i-texnika/163629-andreeva-l-e-uprugie-elementy-priborov.html>
3. Shimyrbaev, M. K. (1992). Utochnennye metody opredeleniya uprugih postoyannykh odnonapravlenno armirovannogo materiala. Alma-Ata, 14.
4. Kurochka, K. S., Stefanovskiy, I. L. (2014). Raschet mnogoslonykh osesimmetrichnykh obolochek metodom konechnykh elementov. Informatsionnye tehnologii i sistemy 2014 (ITS 2014): materialy mezhdunarodnoy nauchnoy konferentsii. Minsk, 214–215. Available at: <https://libeldoc.bsuir.by/bitstream/123456789/2008/2/%d0%a0%d0%b0%d1%81%d1%87%d0%b5%d1%82%20%d0%bc%d0%bd%d0%be%d0%b3%d0%be%d1%81%d0%bb%d0%be%d0%b9%d0%bd%d1%8b%d0%b9%20%d0%be%d1%81%d0%b5%d1%81%d0%b8%d0%bc%d0%bc%d0%b5%d1%82%d1%80%d0%b8%d1%87%d0%bd%d1%8b%d1%85%20%d0%be%d0%b1%d0%be%d0%bb%d0%be%d1%87%d0%b5%d0%ba.PDF>
5. Golova, T. A., Andreeva, N. V. (2019). Analysis of methods of calculation of layered plates and shells for the calculation of multilayer structures. The Eurasian Scientific Journal, 5. Available at: <https://esj.today/PDF/41SAVN519.pdf>
6. Bazhenov, V. A., Solovei, N. A., Krivenko, O. P., Mishchenko, O. A. (2014). Modeling of nonlinear deformation and buckling of elastic inhomogeneities shells. Stroitel'naya mehanika inzhenernykh konstruktsiy i sooruzheniy, 5, 14–33. Available at: <https://cyberleninka.ru/article/n/modelirovanie-nelineynogo-deformirovaniya-i-poteri-ustoychivosti-uprugih-neodnorodnykh-obolochek>
7. Kairov, A. S., Vlasov, O. I., Latanskaya, L. A. (2017). Free vibrations of constructional non-homogeneous multilayer orthotropic composite cylindrical shells. Visnyk Zaporizkoho natsionalnoho universytetu. Fizyko-materatychni nauky, 2, 57–65. Available at: <http://eir.nuos.edu.ua/xmlui/bitstream/handle/123456789/4559/Kairov%205.pdf?sequence=1&isAllowed=y>



8. San'kov, P., Tkach, N., Voziiian, K., Lukianenko, V. (2016). Composite building materials and products. *International scientific journal*, 4 (1), 80–82. Available at: [http://nbuv.gov.ua/UJRN/mnj\\_2016\\_4\(1\)\\_24](http://nbuv.gov.ua/UJRN/mnj_2016_4(1)_24)
9. Marasulov, A., Safarov, I. I., Abdramova, G. A., Tolep, A. S. (2021). Own vibrations of ribbed truncated conical shell. *Vestnik KazNRTU*, 143 (3), 211–221. doi: <https://doi.org/10.51301/vest.su.2021.i3.28>
10. Potapov, A. N. (2018). About the free-vibration mode shapes of elastoplastic dissipative systems. *International Journal for Computational Civil and Structural Engineering*, 14 (3), 114–125. doi: <https://doi.org/10.22337/2587-9618-2018-14-3-114-125>
11. Yankovskii, A. P. (2020). The Refined Model of Viscoelastic-Plastic Deformation of Reinforced Cylindrical Shells. *PNRPU Mechanics Bulletin*, 1, 138–149. doi: <https://doi.org/10.15593/perm.mech/2020.1.11>
12. Bakulin, V. N. (2019). Posloyniy analiz napryazhenno-deformirovannogo sostoyaniya trehsloynnykh obolochek s vyrezami. *Izvestiya Rossiyskoy Akademii Nauk. Mehanika Tverdogo Tela*, 2, 111–125. doi: <https://doi.org/10.1134/s0572329919020028>
13. Senjanović, I., Čakmak, D., Alujević, N., Čatipović, I., Vladimir, N., Cho, D.-S. (2019). Pressure and rotation induced tensional forces of toroidal shell and their influence on natural vibrations. *Mechanics Research Communications*, 96, 1–6. doi: <https://doi.org/10.1016/j.mechrescom.2019.02.003>
14. Bazhenov, V. A., Luk'yanchenko, O. A., Vorona, Y. V., Kostina, E. V. (2018). Stability of the Parametric Vibrations of a Shell in the Form of a Hyperbolic Paraboloid. *International Applied Mechanics*, 54 (3), 274–286. doi: <https://doi.org/10.1007/s10778-018-0880-4>
15. Ajarmah, B., Shitikova, M. (2019). Numerical analysis of nonlinear forced vibrations of a cylindrical shell with combinational internal resonance in a fractional viscoelastic medium. *IOP Conference Series: Materials Science and Engineering*, 489, 012033. doi: <https://doi.org/10.1088/1757-899x/489/1/012033>
16. Yang, S. W., Zhang, W., Mao, J. J. (2019). Nonlinear vibrations of carbon fiber reinforced polymer laminated cylindrical shell under non-normal boundary conditions with 1:2 internal resonance. *European Journal of Mechanics - A/Solids*, 74, 317–336. doi: <https://doi.org/10.1016/j.euromechsol.2018.11.014>
17. Lugovoi, P. Z., Sirenko, V. N., Prokopenko, N. Y., Klimenko, K. V. (2017). Influence of the Parameters of a Non-Constant Disturbing Load on the Transient Process of Vibrations of a Ribbed Cylindrical Shell. *International Applied Mechanics*, 53 (6), 680–687. doi: <https://doi.org/10.1007/s10778-018-0850-x>
18. Tornabene, F., Fantuzzi, N., Baccocchi, M. (2017). A new doubly-curved shell element for the free vibrations of arbitrarily shaped laminated structures based on Weak Formulation IsoGeometric Analysis. *Composite Structures*, 171, 429–461. doi: <https://doi.org/10.1016/j.compstruct.2017.03.055>